Mon. Not. R. astr. Soc. (1976) **174**, 455–466.

AN APERTURE SYNTHESIS STUDY OF H I IN THE IRREGULAR II GALAXY NGC 3077

G. A. Cottrell

Mullard Radio Astronomy Observatory, Cavendish Laboratory, Cambridge

(Communicated by J. E. Baldwin)

(Received 1975 July 21; in original form 1975 April 18)

SUMMARY

The Cambridge Half-Mile telescope has been used in conjunction with a 160-channel cross-correlation receiver to map the neutral hydrogen emission in NGC 3077 with a synthesized beam of width $1'{\cdot}5 \times 1'{\cdot}6$. The H I distribution is found to be severely distorted, with the projected centroid lying about 4 kpc SE of the optical centre in a region where star formation may be occurring, and a streamer of H I extending ~ 10 kpc northwards. The observed H I mass is $4{\cdot}1 \times 10^8\ M_\odot$ of which a quarter is in the streamer. A small gradient of radial velocity exists across the galaxy which, if interpreted as rotation, suggests an indicative mass of $(6 \pm 2) \times 10^9\ M_\odot$. A computer model is proposed to explain the distorted H I distribution in terms of tidal forces exerted during a close (12 kpc) encounter between NGC 3077 and M81, (2 to 6) $\times$ 10^8 yr ago.

1. INTRODUCTION

NGC 3077 is an Irr II galaxy with small ellipticity and the major axis in position angle 45°. There is a good illustration of it in the *Hubble Atlas of Galaxies* (Sandage 1961). The Holmberg (1958) dimensions, which correspond to a limiting isophote of brightness 26·5 mag (arcsec)$^{-2}$, are $8'{\cdot}8 \times 8'$ but on a deep (baked) IIIa–J+WC2 plate (Barbieri, Bertola & di Tullio 1974) the maximum diameter is 10′. Several dust lanes, characteristic of Irr II galaxies, extend radially to the NW edge. A tangled system of Hα filaments (Barbieri *et al.* 1974) lies within about 1′ of the nucleus and on a blue plate there is a wide absorption region crossed by a thin filament, together with a number of bright knots, the brightest of which they assume to be the nucleus.

NGC 3077 is a member of the M81 group, having as its closest companions M81, 48′ away, and M82, 70′ away. Tammann & Sandage (1968) find a distance modulus of 27·55 ($\equiv 3{\cdot}25$ Mpc) for the M81 group, and this value is adopted here for NGC 3077; 1′ then corresponds to 945 pc. The three galaxies M81, M82 and NGC 3077 are embedded in a diffuse H I halo (Roberts 1972). M81 is an Sb galaxy recently mapped in H I by Gottesman & Weliachew (1975) and Rots & Shane (1974), whereas M82 has an optical texture very similar to that of NGC 3077 and is also classified as an Irr II galaxy. It contains a continuum radio source, most recently mapped by Hargrave (1974) with the Cambridge 5-km telescope at 5 GHz. Irr II galaxies are rare and it is therefore noteworthy that two such galaxies belong to the same dynamical group.

This paper describes observations (Section 2), made with the Half-Mile telescope at the Mullard Radio Astronomy Observatory, of the hydrogen distribution and velocity field in NGC 3077. The results are presented in Section 3 and are then discussed in Section 4, particularly in relation to the dynamics of the M81/M82/NGC 3077 group and a possible tidal interaction of NGC 3077 with M81.

2. OBSERVATIONS AND DATA REDUCTION

Application of the Half-Mile telescope to the mapping of H I in external galaxies has been described in an earlier paper (Baldwin *et al.* 1971). Observations were made in the period 1974 January–March and consisted of 12-hr runs at each of 60 interferometer spacings, the incremental spacing being 6·1 m. The corresponding half-power widths of the synthesized beam were 1′·5 in right ascension by 1′·6 in declination, equivalent to 1·3 kpc by 1·4 kpc at the assumed distance of NGC 3077. The smallest spacing present was 12·2 m (58 λ), so source structure of angular extent greater than 1° will be missing from the maps. The receiver phase and sensitivity were calibrated at each spacing by observations of 3C 309.1, the flux density of which was taken to be 7·9 Jy ($7{\cdot}9 \times 10^{-26}$ W m^{-2} Hz^{-1}) (Kellermann, Pauliny-Toth & Williams 1969). The noise temperature of the system was 120 K.

Line profiles were measured by a 160-channel digital cross-correlation spectrometer operating at a bandwidth of 4 MHz centred at 1420·4 MHz. The peaks of the single-channel response curves were 125 kHz apart (corresponding to a Doppler shift of 26·4 km s^{-1}) and the half-power points of each channel have a frequency separation of 150 kHz. The frequency-sidelobe levels are less than 5 per cent of the maximum value. Broadband (10 MHz) radiation centred at 1420·4 MHz was simultaneously recorded on a separate receiver. Typical daily variations in the sensitivity scales of both receivers were less than 5 per cent. The raw data were stored on punched-paper tape and processed on the IBM 370/165 at the University Computer Laboratory.

Single-channel maps containing both line and broadband radiation were prepared for a number of channels. The measured rms noise temperature was found to be 1·6 K, close to the theoretical value of 1·4 K. After identifying those maps containing significant line emission, a further map was made by averaging the remaining single-channel outputs within the velocity ranges 417 to 153 and -375 to -85 km s^{-1} (giving a total bandwidth of 2·6 MHz). This map was then subtracted from the single-channel maps to provide maps of the H I alone. The rms noise on the subtracted maps is 1·7 K. A map of the integrated H I was also produced, all values on the continuum-free single-channel maps less than $1{\cdot}5 \times$ rms noise level being set to zero before summation.

3. RESULTS

The three single-channel maps showing the most H I emission are presented in Fig. 1(a)–(c). The contour interval is in units of the rms noise level σ (1·7 K), the lowest contour (dashed) being 1 σ. The narrow dashed line corresponds to the Holmberg boundary (8′·8 × 8′) centred on the optical position given by Gallouët, Heidmann & Dampierre (1973), i.e. $\alpha = 09^h\,59^m\,21^s{\cdot}5 \pm 3^s$, $\delta = 68°\,58'\,31'' \pm 5''$ (1950·0) which is marked by a +. The radial velocities marked on each map have

1976MNRAS.174..455C

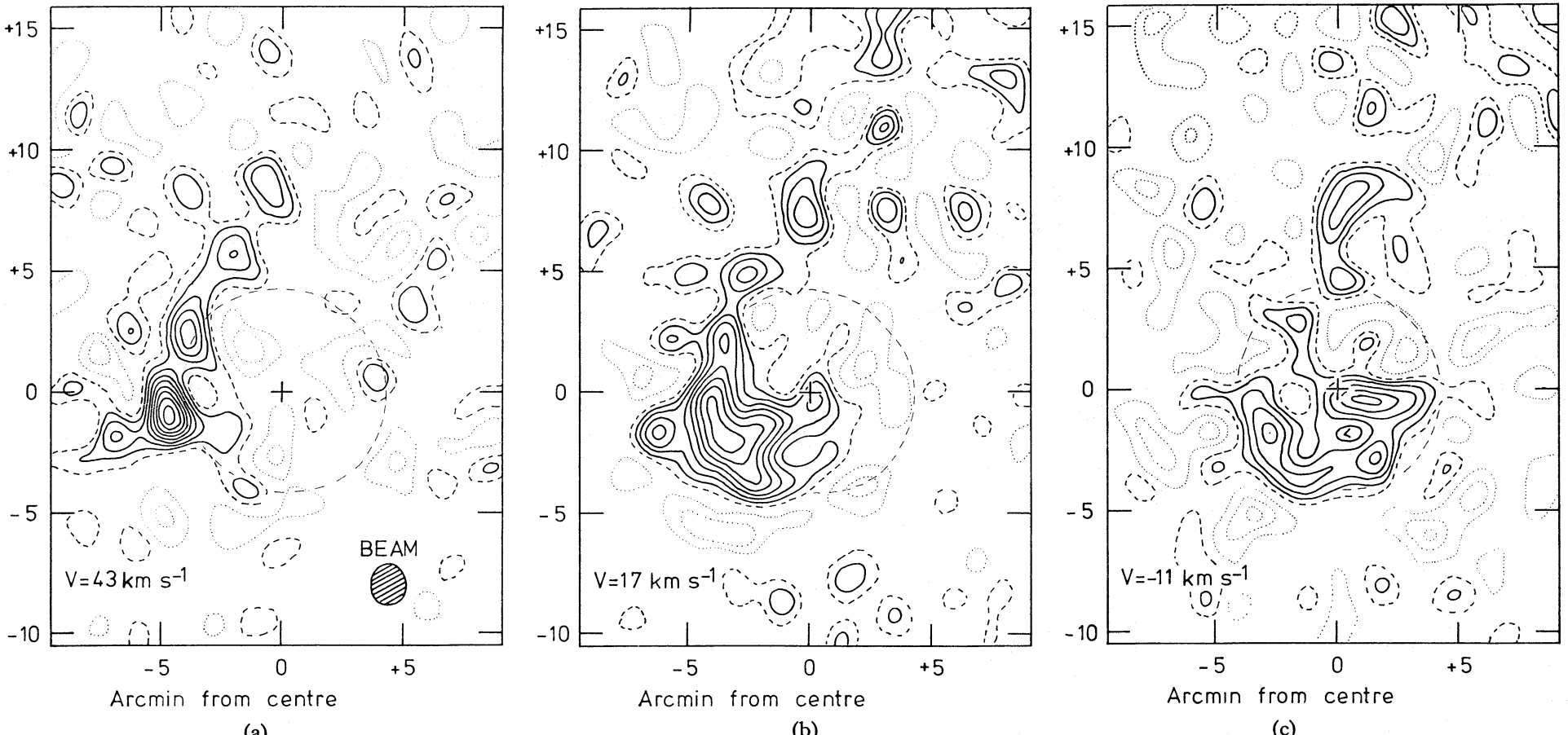

FIG. 1(*a*)–(*c*). *Three continuum-free single-channel maps of H* I *emission in NGC* 3077. *In each map the contour interval is the same* (1·7 *K*). *V denotes the heliocentric radial velocity. The dashed line represents the Holmberg boundary. The hatched ellipse, in Fig.* 1(*a*), *is the synthesized beamshape. The dotted lines are negative contours.*

been corrected to heliocentric values. The H I absorption in our Galaxy was estimated by measuring the flux density of M82 in all of the original single-channel maps; since variations in the apparent flux density were less than 4 per cent (consistent with Rots & Shane 1974) no corrections were applied. From the broad-band continuum map, the flux density of the nuclear source in NGC 3077 was found to be $(23 \pm 3) \times 10^{-3}$ Jy. It was unresolved ($\lesssim 1'{\cdot}5$) and is at the position $\alpha = 09^h\ 59^m\ 17^s \pm 3^s$, $\delta = 68°\ 58'\ 31'' \pm 8''$ (1950·0), results confirming those of van der Kruit (1971) who found an unresolved source ($\leqslant 7''$) of flux density 21×10^{-3} Jy at 1415 MHz coincident with one of the blue knots at $\alpha = 09^h\ 59^m\ 19^s{\cdot}65$, $\delta = 68°\ 58'\ 31''{\cdot}9$ (1950·0). From the present data it is not possible to measure H I absorption in the nuclear source on the single-channel maps because its brightness temperature is less than the peak brightness temperature of the H I.

The integrated H I profile was found by the following method. In the area of sky enclosed by the outer H I contour on the integrated hydrogen map (Fig. 3) the total flux density for each single-channel map was measured. This was then plotted (Fig. 2) against radial velocity. The total mass of optically thin H I observed in emission was determined by integrating under the curve of Fig. 2. The value was $(4{\cdot}1 \pm 0{\cdot}2) \times 10^8\ M_\odot$ whereas Lewis & Davies (1973) found a mass of $(6{\cdot}1 \pm 0{\cdot}6) \times 10^8\ M_\odot$. The difference between these values could be due to the higher noise level in the present observations hiding extended H I of low surface brightness, possibly a part of the extended H I envelope observed by Roberts (1972).

The mean velocity of the H I is indicated by the arrow on Fig. 2, namely (15 ± 5) km s^{-1}, and was taken to be the systemic H I velocity of NGC 3077. This

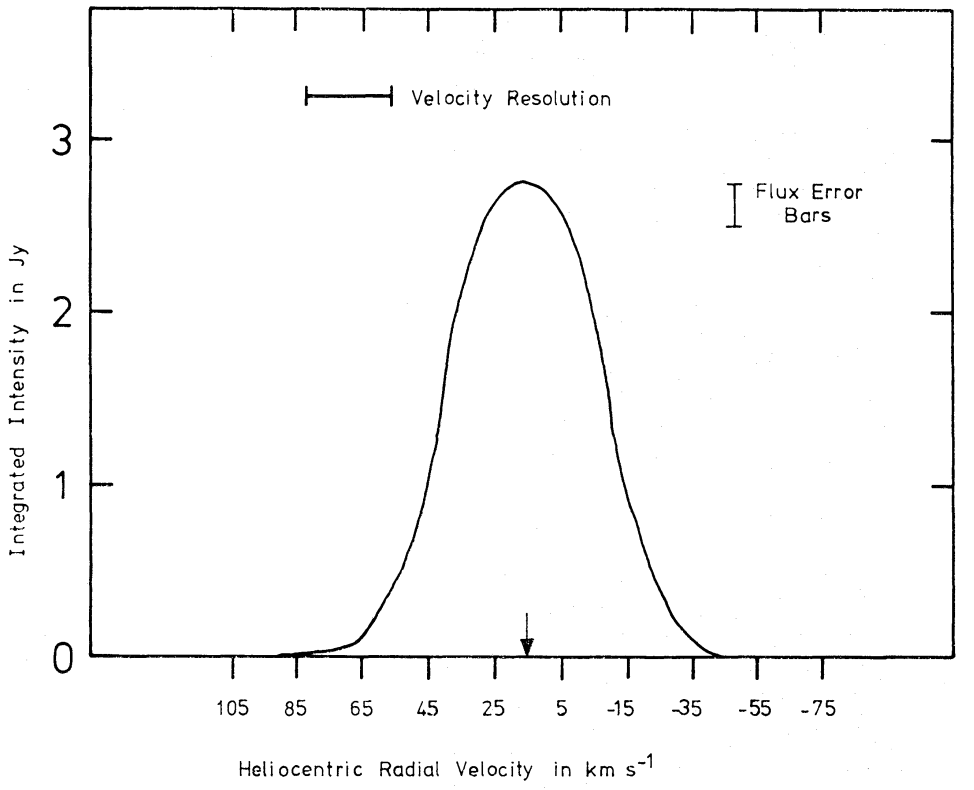

FIG. 2. *The integrated spectrum of H I emission derived by the method described in the text. The arrow shows the mean velocity weighted by flux density, namely* 15 ± 5 *km s*$^{-1}$.

value is in good agreement with the H I systemic velocity of 10 km s^{-1} quoted by Lewis & Davies (1973), but Demoulin (1969) and Barbieri *et al.* (1974) give the optical radial velocity as -10 km s^{-1}.

The integrated H I map is shown in Fig. 3. The observed mass of H I inside the Holmberg boundary is $2{\cdot}4 \times 10^8 M_\odot$ (58 per cent of the total), while $0{\cdot}9 \times 10^8 M_\odot$ (21 per cent of the total) lies in the northern condensation and associated bridge outside the Holmberg boundary.

4. DISCUSSION

4.1 *The H I distribution*

Inspection of Fig. 3 shows the distribution of hydrogen to be extremely unsymmetrical with respect to the Holmberg boundary and the optical centre. There is a striking lack of H I emission from the main distribution of stars, the projected centre of H I emission lying roughly 4′ (~4 kpc) in pa 125° ± 10° from the optical nucleus. Two large complexes of H I, together contributing 10 per cent of the total H I emission, are in this region with a third complex nearly 10′ north of the optical nucleus. Coincident with the southern half of the Holmberg boundary is a roughly semicircular plateau of H I which seems to be slightly extended towards

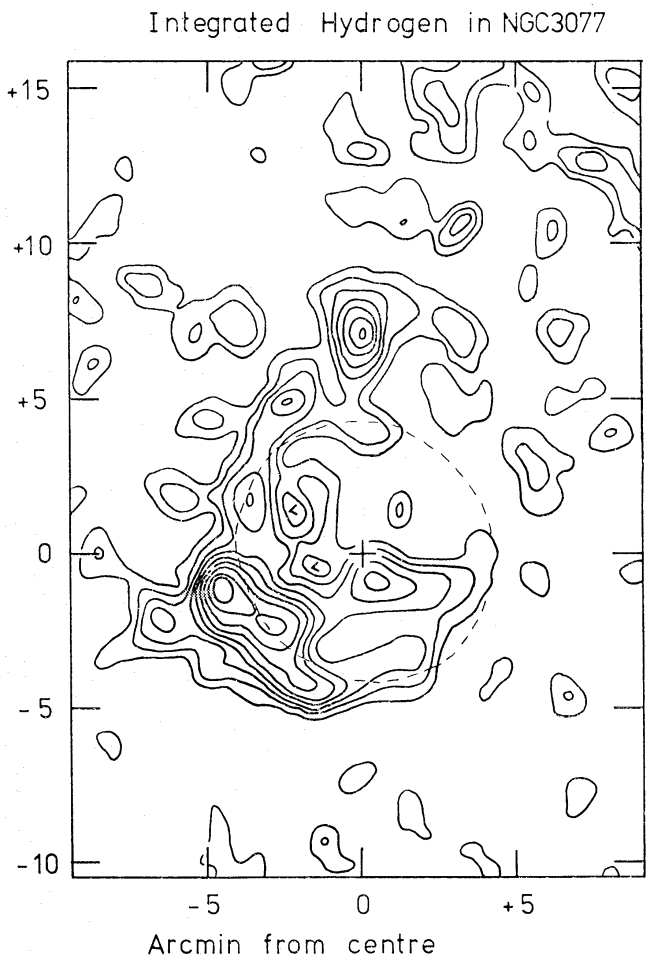

FIG. 3. *The integrated H I map. The first contour is 47 K km s^{-1} and subsequent contours are spaced equally above this level by 94 K km s^{-1}. The dashed line is the Holmberg boundary, and the rms noise is 42 K km s^{-1}.*

the east. Connecting the northern complex to the plateau region is a low-brightness filament containing some partially-resolved condensations. The mean projected surface density of H I in the filament is 4×10^{20} atom cm^{-2}.

At $\alpha \approx 09^h\,59^m\,48^s$, $\delta \approx 68°\,56'\,14''{\cdot}9$ (1950·0), about 4′ SE of the optical nucleus, Barbieri *et al.* (1974) have found a group of stellar objects rather like a Magellanic galaxy of low surface brightness. They lie in a region of high H I surface density ($1{\cdot}2 \times 10^{21}$ atom cm^{-2}), about 37″ (580 pc) SW of one of the large complexes which is at the position $\alpha = 09^h\,59^m\,52^s{\cdot}6 \pm 3^s$, $\delta = 68°\,56'\,43''{\cdot}2 \pm 8''$ (1950·0). Barbieri *et al.* suggest that star formation might be taking place in this region and the association of H I with this group adds weight to the idea. If the H I distribution is ~1 kpc thick in the line of sight, then the volume density of H I in the region of the stars is ~0·5 atom cm^{-3}. No stellar condensations have been found associated with the northern streamer and there appears to be little H I associated with the dust lanes near the NW edge.

4.2 *The velocity field*

Examination of the single-channel maps in Fig. 1 shows the centroid of the H I emission to be displaced in a systematic manner according to radial velocity. This could be interpreted as being due to galactic rotation. An isovelocity contour map of NGC 3077 is shown in Fig. 4 to demonstrate this effect more clearly. This map

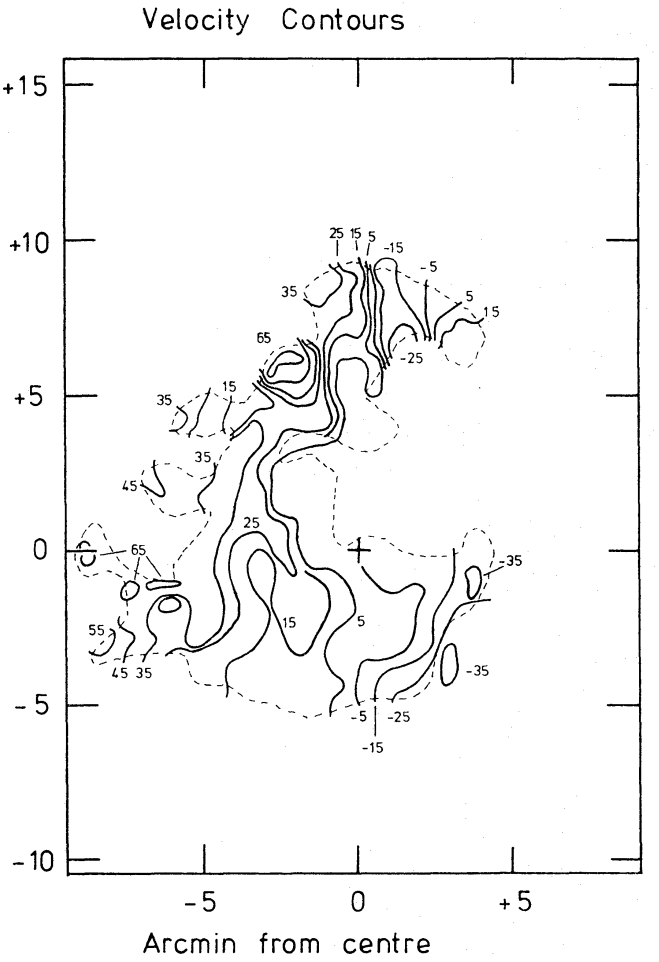

FIG. 4. *An isovelocity map (solid contours) of NGC 3077. The velocity of each contour is in km s^{-1} with respect to the Sun. The dashed line is the outer H I contour taken from Fig. 3.*

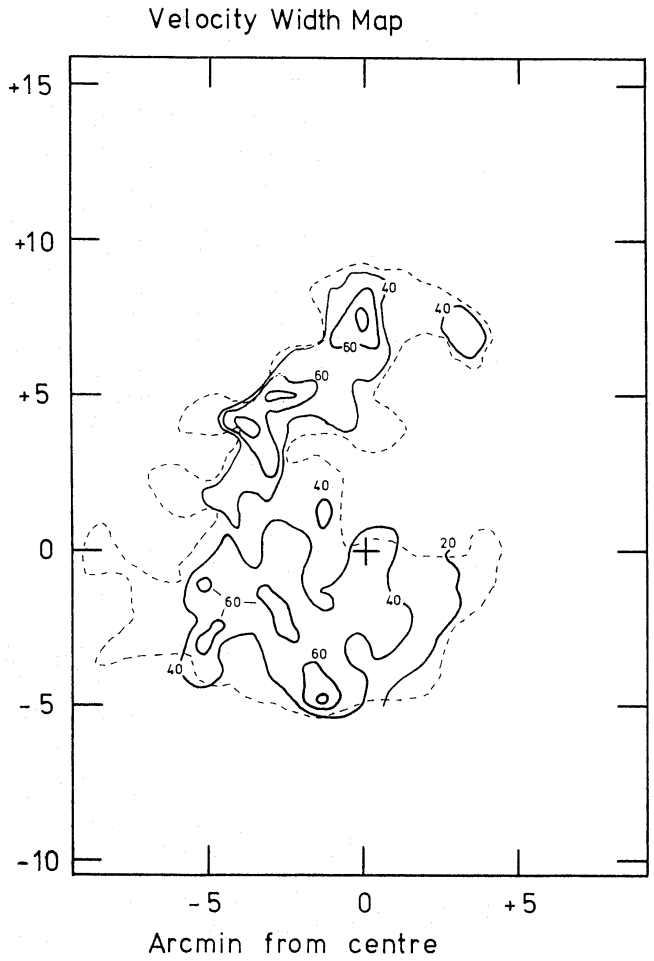

FIG. 5. *A velocity-width map constructed by finding the full width at half-maximum intensity of the H I emission profile at each map point. The contour interval is 20 km s^{-1}, and the dashed line is the outer H I contour taken from Fig. 3.*

was made from the mean velocities of the H I profiles. These were calculated by finding the velocities at which a profile had fallen to half the peak height and taking the mean to give a characteristic radial velocity for the profile. The full width to half intensity of the profile indicates the velocity dispersion within one beam area, and a map of the velocity widths (Fig. 5) shows the observed values uncorrected for an instrumental broadening of 31·6 km s^{-1}.

The H I velocity gradient seems to have its greatest value close to the direction of the optical major axis (pa = 45°) and in the sense that the eastern sector of the galaxy is receding from the observer. The maximum radial-velocity difference observed in the galaxy is ~100 km s^{-1} and rotation occurs over a distance of 13′ (~13 kpc). The northern streamer has a range of radial velocities which are continuous with those in the galaxy. The velocity gradient across the width of the streamer is ~40 km s^{-1} kpc^{-1}, and the velocity dispersion in the northern complex is ~75 km s^{-1}.

By assuming the gas to be moving in circular motion around a central mass point, we can estimate the mass, M, for NGC 3077 from the formula

$$M = (V_m^2 R_m/G)\,\mathrm{cosec}^2\, i,$$

where V_m is half the maximum velocity range over which H I is observed, R_m

is the maximum radius at which H I is observed and i is the inclination between the rotational axis and the line of sight. If NGC 3077 is a flat disc, the mean axial ratio of 0·7 leads to a value $i = 46°$. We can define the true axial ratio, ϵ_T, of a galaxy by assuming that the galaxy is an oblate spheroid with inclination i having apparent axial ratio, ϵ_A, where

$$\cos^2 i = (\epsilon_A{}^2 - \epsilon_T{}^2)/(1 - \epsilon_T{}^2).$$

Table I shows the range of masses, hydrogen-to-total-mass ratios (M_H/M), mass-to-light ratios (M/L) and inclinations (i) for various values of the true axial ratio (ϵ_T). Hodge & Hitchcock (1966) have concluded that most irregular galaxies have true axial ratios in the range 0·2–0·4 and parameters corresponding to these ratios are included in the table as well as the edge-on case $i = 90°$.

TABLE I

ϵ_T	Inclination i (°)	Mass M ($10^9 M_\odot$)	M_H/M	M/L
0	46	7·4	0·05	4·5
0·2	47	7·1	0·06	4·3
0·4	51	6·2	0·07	3·7
0·7	90	3·8	0·11	2·3

Lewis & Davies (1973) derive a photographic luminosity for NGC 3077 of $1{\cdot}65 \times 10^9 L_\odot$ corrected to infinite radius and residual face-on absorption. The M/L ratios in Table I assume this value. These authors also quote a corrected colour index of 0·67. Using the H I mass found in this survey, the distance-independent parameter of H I mass to luminosity is 0·25.

4.3 *The dynamics of M81, M82 and NGC 3077*

The dynamical data for the trio consist of the masses and radial velocities of the individual galaxies and are summarized in Table II.

TABLE II

Galaxy	Mass ($10^9 M_\odot$)	Radial velocity (km s^{-1})
M81	110*	-31 ± 6*
M82	10 ± 5†	240‡
NGC 3077	6 ± 2	15 ± 5

* Gottesman & Weliachew (1975).
† Burbidge, Burbidge & Rubin (1964).
‡ Heckathorn (1972).

In making the following estimates, no account has been taken of the H I 'halo' discovered by Roberts (1972) and it is assumed that the main interacting masses are the galaxies themselves. The projected distance of M82 from M81 is ≈ 38 kpc and at this distance the escape velocity from M81 is 169 km s^{-1}. Since M82 has a radial velocity of 271 km s^{-1} with respect to M81, this pair cannot be bound unless there is a great deal ($\sim 3 \times 10^{11} M_\odot$) of unobserved matter near M81. If we consider the pair M81–NGC 3077, however, the difference in the radial velocities is

only ≈ 46 km s^{-1} and they seem likely to be bound. From the projected distance, the dynamical free-fall time of NGC 3077 to M81 is $\sim 5 \times 10^8$ yr.

4.4 *Tidal interaction and NGC 3077*

Any model of the highly disturbed H I distribution must be able to account for the following observational features:

(a) The projected centroid lies $\sim 4'$ SE of the optical centre;

(b) an H I complex lies $\approx 10'$ north of the optical centre and is connected to the main body of H I by a diffuse and slightly curved bridge of neutral hydrogen with width ≈ 2 kpc and mean surface density 4×10^{20} atom cm^{-2}; and

(c) the velocity dispersion associated with the northern complex is ≈ 70 km s^{-1}, and the gradient in the bridge is ≈ 40 km s^{-1} kpc^{-1}. In interpreting these features it is natural to consider the possibility of a tidal interaction between NGC 3077 and its companion galaxies. In a close encounter, tidal forces will disrupt the outer gaseous regions of a galaxy more than the inner parts where the differential force is smaller.

It can be seen from Table II that the mass of M81 is roughly one order of magnitude greater than that of M82. Both this and the fact that the projected M82–NGC 3077 distance is nearly twice the M81–NGC 3077 distance suggests that M81 has caused the tidal disruption. We have already noted in Section 4.3 that M81 and NGC 3077 may be a bound pair. Rots & Shane (1974) find that the north and south H I rotation curves of M81 are in good agreement out to a radius of ≈ 10 kpc, but beyond this radius the curves deviate significantly and non-circular motions become important. If there was a close encounter between M81 and NGC 3077, it is unlikely that NGC 3077 passed closer than ~ 10 kpc from the centre of M81.

Following the approach of Toomre & Toomre (1972) and others, a computer simulation has been carried out (S. F. Gull, private communication) and is interpreted here as a possible model for NGC 3077. The model assumes that the H I always belonged to NGC 3077 and was originally uniformly distributed in a disc of diameter ≈ 8 kpc coincident with the stellar disc. A disc of 200 massless test particles was set rotating in a parabolic potential well and the evolution of the disc was studied as it performed a coplanar parabolic trajectory about a second point mass having 10 times the mass of the first. Various stages of the encounter are shown in Fig. 6, the perigalacticon distance being 12 kpc.

In the simulation of Fig. 6, which is pictured in the plane of the collision, the test particles rotate in a *retrograde* sense with respect to the orbital angular momentum, but in the corresponding collision with prograde rotation, most of the particles were pulled off the companion, approximately half being captured by the central mass, the other half escaping from the system entirely. It is important to note that for a retrograde collision of the type considered in this model, the formation of a single tail is a broad phenomenon which is independent of the exact details of collision over a large range of parameter space. In Fig. 6, the time step, t, is in units of 10^8 yr. Soon after perigalacticon, a single tail forms which persists for 7×10^8 yr before breaking up. From the ratio of the tail length to the separation between the companion and central galaxies, we can identify the stage in the collision that NGC 3077 has reached. The observed ratio is $\approx 0{\cdot}3$ which corresponds with the time $t = 8$ to $t = 10$ in Fig. 6, though at $t = 9$ the tip of the tail

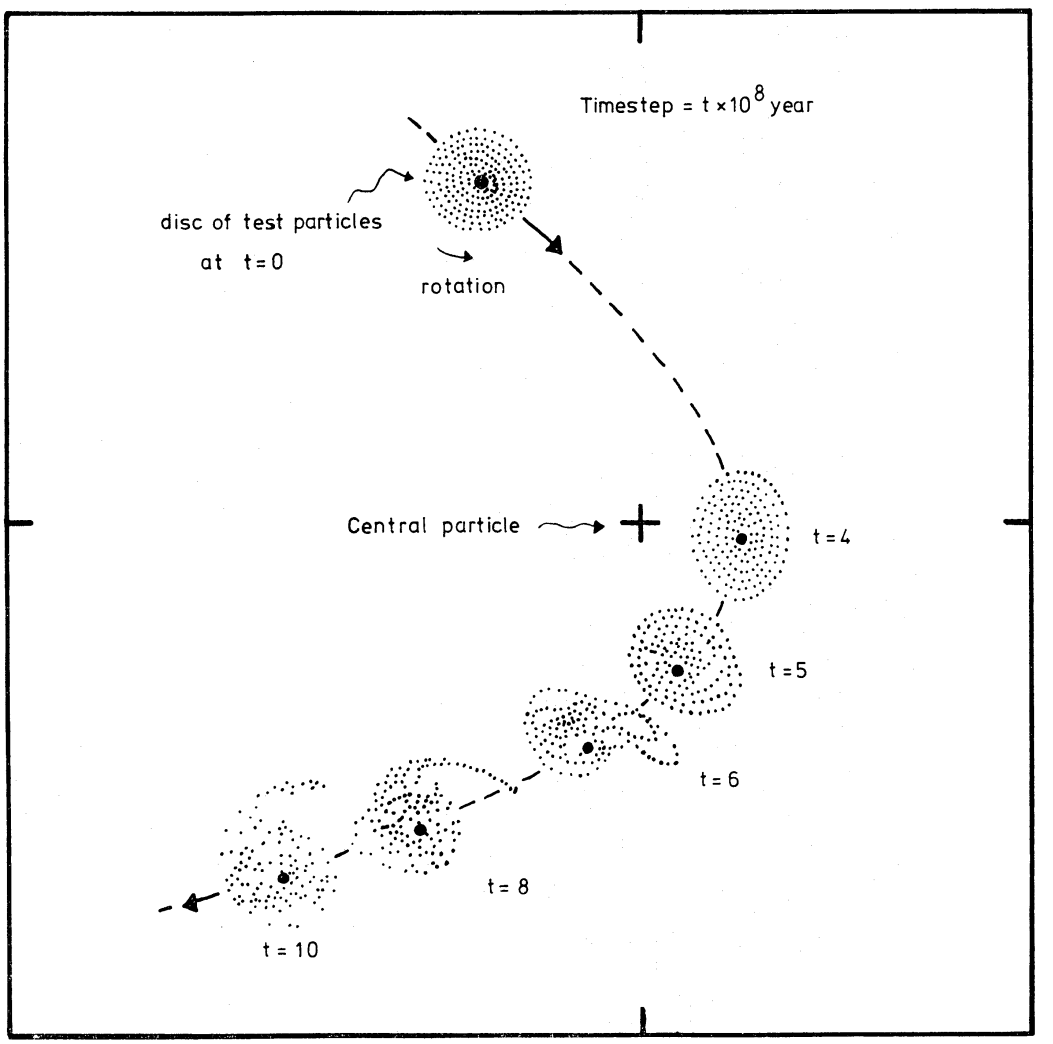

FIG. 6. *A computer simulation showing the distortion of a disc of massless test particles rotating in a parabolic potential well during a coplanar, parabolic, close encounter with a second point mass. The centre of the companion galaxy's potential well is marked at various times, t, in the collision by the series of black points lying on the parabola (dashed line). The time interval, t, is in units of* 10^8 *yr.*

crosses above the line joining the two galaxies. Thus the closest approximation of the present orientation of the tail occurs at a time 6×10^8 yr after perigalacticon. However, at an earlier time $t = 6$, the model best simulates the displacement of the test particles to the east side of the companion galaxy. On this basis, the time since perigalacticon turns out to be $t = 2 \times 10^8$ yr. To relate Fig. 6 to the orbit as seen on the plane of the sky, the page should be viewed tilted on a horizontal axis with the top half nearer the reader so as to make an inclination of about 50°.

The radial velocity gradient across the tail of NGC 3077 is ≈ 40 km s^{-1} kpc^{-1} (Fig. 4). If the tail is only ≈ 2 kpc thick, then it will double its width in a time $\sim 5 \times 10^7$ yr. The persistence of the tail for longer times (~ 8 few$\times 10^8$ yr) may indicate that it is a sheet or loop of H I seen edge-on. In the simulation the velocity dispersion in the tail cannot be very large compared with that of the galaxy, and the 2-D model as it stands cannot easily explain the longevity and the range of velocities in the real tail. A more refined simulation with particle motions in the third dimension may shed more light on these features. A striking feature of the

deep plate of Barbieri *et al.* (1974) is that there is no low brightness optical emission associated with the streamer, whereas the collision simulations by Clutton-Brock (1972), performed with a self-gravitating stellar component plus a gaseous component of low velocity-dispersion, show that both stars and gas are affected similarly by tides. It may be that there is a stellar tail to NGC 3077 but we cannot see it. No stars have yet been detected in the 'Magellanic Stream' (Mathewson, Cleary & Murray 1974).

If the tidal interaction picture is essentially correct and the angle between the angular momentum vector of NGC 3077 and the orbital angular momentum is close to 180°, then both the condition of retrograde rotation in the model, and the fact that the eastern half of NGC 3077 is receding from the observer, imply unambiguously that NGC 3077 is now farther from us than M81. This means that the parabolic orbit of Fig. 6 has to be inclined such that NGC 3077 is now moving away from us with a higher systemic velocity relative to M81. This prediction is in agreement with the facts of Table II but it is difficult to calculate the inclination of the orbit precisely—in the model it is at least as uncertain as the inclination of NGC 3077 itself.

Two main lines of future research are suggested by this work:

(a) A search for optical emission from the streamer; and
(b) a more refined 3-D computer model.

ACKNOWLEDGMENTS

I thank many members of the Radio Astronomy Group for assistance with the observations and Mrs R. E. Walker and Mrs S. A. Jongsma for help in reducing the data. In particular I thank Dr J. E. Baldwin and Dr J. R. Shakeshaft for valuable discussions and help with the manuscript. I am also indebted to S. F. Gull for use of his computer simulation results.

REFERENCES

Baldwin, J. E., Field, C., Warner, P. J. & Wright, M. C. H., 1971. *Mon. Not. R. astr. Soc.*, **154**, 445.
Barbieri, C., Bertola, F. & di Tullio, G., 1974. *Astr. Astrophys.*, **35**, 463.
Burbidge, E. M., Burbidge, G. R. & Rubin, V. C., 1964. *Astrophys. J.*, **140**, 942.
Clutton-Brock, M., 1972. *Astrophys. Space Sci.*, **17**, 292.
Demoulin, M.-H., 1969. *Astrophys. J.*, **157**, 81.
Gallouët, L., Heidmann, N. & Dampierre, F., 1973. *Astr. Astrophys. Suppl.*, **12**, 1.
Gottesman, S. T. & Weliachew, L., 1975. *Astrophys. J.*, **195**, 23.
Hargrave, P. J., 1974. *Mon. Not. R. astr. Soc.*, **168**, 491.
Heckathorn, H. M., 1972. *Astrophys. J.*, **173**, 501.
Hodge, P. W. & Hitchcock, J. L., 1966. *Publ. astr. Soc. Pacific*, **78**, 79.
Holmberg, E., 1958. *Medd. Lunds astr. Obs.*, Ser. II, No. 136.
Kellermann, K. I., Pauliny-Toth, I. I. K. & Williams, P. J. S., 1969. *Astrophys. J.*, **157**, 1.
Lewis B. M. & Davies, R. D., 1973. *Mon. Not. R. astr. Soc.*, **165**, 213.
Mathewson, D. S., Cleary, M. N. & Murray, J. D., 1974. In *The formation and dynamics of galaxies*, IAU Symp. No. 58, p. 367, ed. J. R. Shakeshaft, D. Reidel Publishing Co., Dordrecht.
Roberts, M. S., 1972. In *External galaxies and quasi-stellar objects*, IAU Symp. No. 44, p. 12, ed. D. S. Evans, D. Reidel Publishing Co., Dordrecht.
Rots, A. H. & Shane, W. W., 1974. *Astr. Astrophys.*, **31**, 245.

Sandage, A., 1961. *The Hubble Atlas of Galaxies*, Carnegie Institution of Washington, Washington, D.C.
Tammann, G. S. & Sandage, A., 1968. *Astrophys. J.*, **151**, 825.
Toomre, A. & Toomre, J., 1972. *Astrophys. J.*, **178**, 623.
van der Kruit, P. C., 1971. *Astr. Astrophys.*, **15**, 110.